JPE 8-1-3

Torque Ripples Minimization of DTC IPMSM Drive for the EV Propulsion System using a Neural Network

Bhim Singh[*], Pradeep Jain[†], A.P.Mittal[**] and J.R.P.Gupta[**]

[*]Department of Electrical Engineering, Indian Institute of Technology, Delhi, New Delhi, India
[†**]Department of Instrumentation and Control Engineering, NSIT, New Delhi, India

ABSTRACT

This paper deals with a Direct Torque Control (DTC) of an Interior Permanent Magnet Synchronous Motor (IPMSM) for the Electric Vehicle (EV) propulsion system using a Neural Network (NN). The Conventional DTC with optimized switching lookup table and three level torque controller generates relatively large torque ripples in an electric vehicle motor drive. For reducing the torque ripples, a three level torque controller is hereby replaced by the five level torque controller. Furthermore, the switching lookup table of the five level torque controller based DTC is replaced with a Neural Network. These DTC schemes of an IPMSM drive are simulated using MATLAB/SIMULINK. The simulated results are compared with the conventional DTC and it is found that the ripples in the torque, as well as in the stator current, are reduced drastically.

Keywords: DTC, Electric vehicle, IPMSM, Neural network

1. Introduction

Energy and environment issues have boosted the development of the electric vehicle [1]. Concerning the environment, electric vehicles can provide emission-free urban transportation. Electric vehicles may include battery operated electric vehicles (BEVs), hybrid electric vehicles (HEVs), and fuel-cell electric vehicles (FCEVs). The requirements for the EV motor drive include: large torque, high speed, high power density, quick response and good dependability [1-2].

The EV consists of the electric motor propulsion system, transmission device, and wheels as shown in Fig. 1. The electric motor propulsion system is the heart of the EV, which consists of the electric motor, its power converter, and an electronic controller. The electric motor drive is configured to respond to a speed reference set by the pedal of the EV, which reflects the torque demand [2]. To accelerate the EV, the reference torque increases. This activates the controller and increases the developed torque. For braking purposes, the electric regenerative braking is employed wherein the negative torque reference is set by the speed controller. The first portion of the brake pedal travel is used to derive a regenerative torque demand; the remaining pedal travel brings in a set of standard mechanical brakes.

Manuscript received Aug. 30, 2007; revised Oct. 29, 2007
[†]Corresponding Author: jainpradeep77@gmail.com
[*]Department of Electrical Engineering, I.I.T., Delhi, India
[**]Dept. of Instrumentation and Control Engineering, N.S.I.T., Sec-3, Dwarka, New Delhi-110075, India

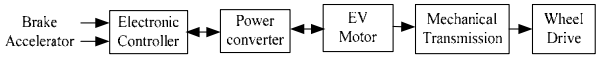

Fig. 1 Electric vehicle composition

DC motors have been prominent in electric propulsion because their torque-speed characteristics suit traction requirement works well and their speed control is simple. Nowadays, the commutatorless motors such as an induction motor (IM), IPMSM and synchronous reluctance machine, are employed with having advantages of high efficiency, high power density, low operating cost, enhanced reliability, and low maintenance over DC motors for the EV propulsion system [2]. Furthermore, considerable interest has emerged in the IPMSM due to its high power density, outstanding efficiency, and potential for quiet operation over the other commutatorless motors [3-4].

The control techniques used for the EV propulsion motor are scalar control, vector control and DTC control. The scalar control is simpler but its accuracy is low and torque response is poor. The vector control exhibits high accuracy, good torque response and wide speed range [5-6]. Furthermore, the vector control provides the torque speed characteristics identical to that of a DC series motor (propulsion motor). But the vector control needs quite complicated coordinate transformations on line to decouple the interaction between flux control and torque control in order to provide fast torque control of the EV propulsion motor. Hence the algorithm computation is time consuming and its implementation usually requires a high performance DSP chip. In recent years an innovative control method called DTC has gained attention for the electric propulsion system [5-7], because it can also produce fast torque control and does not need heavy computation on-line, in contrast to the vector control. The basic principle of DTC is to directly select optimum inverter switching states according to the differences between the references of torque and stator flux linkage and their actual values [5-7]. The current controller followed by a PWM comparator is not used in DTC systems and the parameters of the motor are also not used except for the stator resistance. Therefore, the DTC possesses advantages such as lower parameter dependence and simpler configuration.

Conventional DTC has a three level torque controller in which there is no method to distinguish between very large error and relatively small error in the torque controller. This results in large torque ripples and a current ripple in conventional DTC [7-8]. These ripples may be minimized by introducing an intermediate stage which is generally known as a five level torque controller [8] and use of a neural network based switching table [9]. In this paper the use of a neural network is proposed to emulate the switching lookup table of the DTC of the IPMSM to obtain the optimal switching patterns. The proposed controller is simulated for a variety of operating conditions of the electric vehicle. The simulated results demonstrate that the proposed control structure improves the performance of the DTC IPMSM drive system in terms of reduced stator current and torque ripples.

2. Direct Torque Control (DTC) Scheme for IPMSM

Direct Torque Control scheme of an IPMSM drive is shown in Fig. 2.

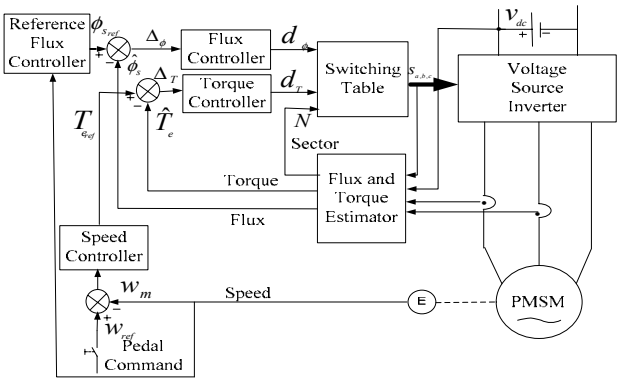

Fig. 2 Conventional Direct Torque Control IPMSM Drive

The DTC controller consists of three components: hysteresis control for torque and flux, an optimal switching vector look-up table and a motor model. The shaft speed (w_m) is compared with the reference speed (w_{ref}). The error in speed is processed in the proportional control (PI) speed controller, which generates the reference torque. This reference torque is limited; using a limiter and limited reference torque (T_{eref}) to generate the torque error by comparing it with the estimated torque of the motor ($\hat{T}_e$). Similarly, flux reference ($\phi_{s_{ref}}$) is obtained from the shaft speed (w_m) of the motor and is compared with the estimated stator flux of the motor ($\hat{\phi}_s$).

The reference torque and flux are compared with their estimated values and control signals are produced by using a torque and flux hysteresis control method. The switching look-up table gives the optimum selection of the switching space vectors for all possible stator flux-linkage space-vector positions based upon the results of flux and torque controllers. In response to these switching space vectors, the VSI controls the winding currents of IPMSM. The motor model estimates the developed torque ($\hat{T}_e$) and stator flux ($\hat{\phi}_s$) based on the sensing of two stator phase currents and the battery voltage (V_{dc}). The phase voltages of the IPMSM are obtained from the switching space vectors of the voltage source inverter (VSI) and the battery voltage (V_{dc}). The speed control of an IPMSM is achieved using a PI speed controller.

2.1 Three Level Torque Controller Based DTC Scheme (Conventional DTC)

There are six non-zero switching space vectors (V_1, V_2,…,V_6) and two zero switching space vectors (V_0, V_7). The switching space vectors are selected using stator flux-linkage space-vector positions and the output of two level flux and three level torque controllers as shown in Fig. 3(a).

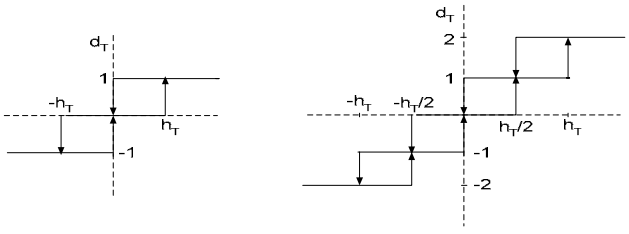

(a) (b)

Fig. 3 (a) Three Level Torque Controller (b) Five Level Torque Controller

Table 1 Switching Table for Three Level Torque Controller DTC Technique

		Sector(N)					
Flux Error	Torque Error	S1	S2	S3	S4	S5	S6
$d_\varphi = 1$	$d_T = 1$	V_2	V_3	V_4	V_5	V_6	V_1
	$d_T = 0$	V_7	V_0	V_7	V_0	V_7	V_0
	$d_T = -1$	V_6	V_1	V_2	V_3	V_4	V_5
$d_\varphi = 0$	$d_T = 1$	V_3	V_4	V_5	V_6	V_1	V_2
	$d_T = 0$	V_0	V_7	V_0	V_7	V_0	V_7
	$d_T = -1$	V_5	V_6	V_1	V_2	V_3	V_4

The corresponding switching look-up table is shown in Table 1.

2.2 Five Level Torque Controller Based DTC Scheme

There are 12 non-zero switching space vectors (V_1, V_2,…,V_6) and "V_{x0}" consisting of "V_x", x = 1, 2,…,6, are synthesized by zero space vectors either V_0 or V_7 and the associated non-zero active switching space vector (V_1, V_2,…,V_6); both have 50% duty and two zero switching space vectors as shown in Fig. 4. The switching space vectors are selected using stator flux-linkage space-vector positions and results in two level flux and five level torque controllers as shown in Fig. 3(b). The corresponding switching look-up table is shown in Table 2.

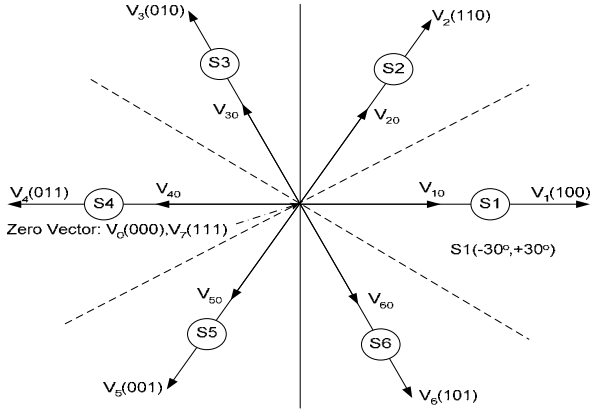

Fig. 4 The Switching Space Vectors and Sectors

Table 2 Switching Table for Five Level Torque Controller DTC Technique

		Sector(N)					
Flux Error	Torque Error	S1	S2	S3	S4	S5	S6
$d_\varphi = 1$	$d_T = 2$	V_2	V_3	V_4	V_5	V_6	V_1
	$d_T = 1$	V_{20}	V_{30}	V_{40}	V_{50}	V_{60}	V_{10}
	$d_T = 0$	V_7	V_0	V_7	V_0	V_7	V_0
	$d_T = -1$	V_{60}	V_{10}	V_{20}	V_{30}	V_{40}	V_{50}
	$d_T = -2$	V_6	V_1	V_2	V_3	V_4	V_5
$d_\varphi = 0$	$d_T = 2$	V_3	V_4	V_5	V_6	V_1	V_2
	$d_T = 1$	V_{30}	V_{40}	V_{50}	V_{60}	V_{10}	V_{20}
	$d_T = 0$	V_0	V_7	V_0	V_7	V_0	V_7
	$d_T = -1$	V_{50}	V_{60}	V_{10}	V_{20}	V_{30}	V_{40}
	$d_T = -2$	V_5	V_6	V_1	V_2	V_3	V_4

2.3 Five Level Torque Controller Based DTC using Neural Network

Here, the switching space vectors are the same as in B. The NN based switching gives the improved selection of the switching space vectors for all possible stator flux-linkage space-vector positions based upon the results of two level flux and five level torque controllers. The five level torque controller based DTC using a neural network scheme of an IPMSM drive is shown in Fig. 5.

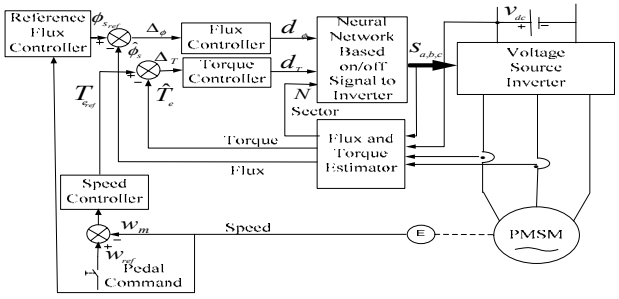

Fig. 5 Neural Network Based DTC IPMSM Drive

3. Motor Modeling and Direct Torque Control Scheme of IPMSM

The basic equations of the direct torque control scheme of an IPMSM drive are given as [3-6], [10].

3.1 PI Speed Controller

The closed loop PI speed controller generates the reference torque $T_{e_{ref}}$ as

$$T_{e_{ref}(n)} = T_{e_{ref}(n-1)} + K_p\left(\Delta w_{m(n)} - \Delta w_{m(n-1)}\right) + K_I \Delta w_{m(n)} \quad (1)$$

where $T_{e_{ref}(n)}$ and $T_{e_{ref}(n-1)}$ are the output of PI speed controller (after limiting it to a suitable value) and $\Delta w_{m(n)}$ and $\Delta w_{m(n-1)}$ refer to speed error at nth and (n-1)th instants. K_p and K_I are proportional and integral gain constants.

3.2 Reference Flux Controller

The reference flux controller generates the reference stator flux as

$$\phi_{s_{ref}} = \begin{cases} \phi_{s\_}, If\ (w_m \le w_{base}) \\ \phi_{s\_}\left(w_{base}/w_m\right), If\ (w_m \rangle w_{base}) \end{cases} \quad (2)$$

where w_m and w_{base} are the shaft speed and base speed of the motor respectively.

3.3 Flux and Torque Controllers

The flux and torque controllers are hystersis type where h_ϕ is the flux hystersis band and h_T is the torque hystersis band. The input to the controllers are the flux error Δ_ϕ and torque error Δ_T and it delivers the control signals d_ϕ and d_T, which represent the voltage demands required to keep the errors within the hystersis band of the controllers. To overcome the torque ripple problem, a five level toque controller is proposed which is shown in Fig. 3(b).

$$\Delta_T \equiv T_{e_{ref}} - \hat{T}_e \quad (3)$$

$$\Delta_\varphi \equiv \phi_{s_{ref}} - \hat{\phi}_s \quad (4)$$

Two level flux controller is as

$$\text{If}\ \Delta_\varphi > h_\varphi, \text{ then } d_\varphi = 1 \quad (5)$$

$$\text{If}\ \Delta_\varphi < -h_\varphi, \text{ then } d_\varphi = 0 \quad (6)$$

Three level torque controller is as

$$\text{If}\ \Delta_T > h_T, \text{ then } d_T = 1 \quad (7)$$

$$\text{If}\ -h_T \le \Delta_T < h_T, \text{ then } d_T = 0 \quad (8)$$

$$\text{If}\ \Delta_T < -h_T, \text{ then } d_T = -1 \quad (9)$$

Five level torque controller is as

$$\text{If}\ \Delta_T >= h_T, \text{ then } d_T = 2 \quad (10)$$

$$\text{If}\ (\Delta_T > h_T/2)\ \&\ (\Delta_T < h_T), \text{ then } d_T = 1 \quad (11)$$

$$\text{If}\ (\Delta_T <= h_T/2)\ \&\ (\Delta_T >= -h_T/2), \text{ then } d_T = 0 \quad (12)$$

$$\text{If}\ (\Delta_T < -h_T/2)\ \&\ (\Delta_T > -h_T), \text{ then } d_T = -1 \quad (13)$$

$$\text{If}\ \Delta_T <= -h_T, \text{ then } d_T = -2 \quad (14)$$

where $\hat{T}_e$ and $\hat{\phi}_s$ are the estimated developed torque and estimated stator flux respectively.

3.4 Direct Torque Control Using Switching Table

A switching table given in Table 1 is used for inverter control so that the torque and flux errors are kept within

the specified bands. The output of the switching table gives the switching state of voltage source inverter. The details of the system are explained as follows.

The d-q axes components of stator voltages are estimated as

$$\begin{bmatrix}\hat{v}_{ds}\\ \hat{v}_{qs}\end{bmatrix}=\frac{V_{dc}}{3}\begin{bmatrix}2 & -1 & -1\\ 0 & \sqrt{3} & -\sqrt{3}\end{bmatrix}\begin{bmatrix}S_a\\ S_b\\ S_c\end{bmatrix} \tag{15}$$

where V_{dc} is the sensed DC link voltage of the inverter (battery voltage) and S_a, S_b, S_c are the switching states of VSI which can take either logic "1" or logic "0".

Similarly the d-q axes components of stator currents are estimated as

$$\begin{bmatrix}\hat{i}_{ds}\\ \hat{i}_{qs}\end{bmatrix}=\frac{1}{3}\begin{bmatrix}2 & -1 & -1\\ 0 & \sqrt{3} & -\sqrt{3}\end{bmatrix}\begin{bmatrix}i_{sa}\\ i_{sb}\\ i_{sc}\end{bmatrix} \tag{16}$$

$$i_{sc}=-(i_{sa}+i_{sc}) \tag{17}$$

where i_{sa} and i_{sb} are the sensed stator currents.

The d-q axes components of stator flux linkages can be estimated by using the estimated d-q axes components of stator voltages and stator currents as.

$$\hat{\phi}_{ds}=\int(\hat{v}_{ds}-\hat{i}_{ds}R_s)dt \tag{18}$$

$$\hat{\phi}_{qs}=\int(\hat{v}_{qs}-\hat{i}_{qs}R_s)dt \tag{19}$$

The estimated flux amplitude is as

$$\hat{\phi}_s=\sqrt{(\hat{\phi}_{ds})^2+(\hat{\phi}_{qs})^2} \tag{20}$$

where R_s is the stator resistance per phase.

The developed torque of the motor is estimated as

$$\hat{T}_e=\frac{3P}{4}(\hat{\phi}_{ds}\hat{i}_{qs}-\hat{\phi}_{qs}\hat{i}_{ds}) \tag{21}$$

3.5 Estimation of Stator Flux-Linkage Space-Vector Positions

The stator flux components are used to obtain the information of stator flux-linkage space-vector positions. These sectors can be determined on the basis of following mathematical relations as

If $\hat{\phi}_{ds}\geq\sqrt{3}\hat{\phi}_{qs}$ *and* $\hat{\phi}_{ds}\geq 0$, then sector = S1 (22)

If $\hat{\phi}_{ds}<\sqrt{3}\hat{\phi}_{qs}$ *and* $\hat{\phi}_{ds}\geq 0$, then sector = S2 (23)

If $|\hat{\phi}_{ds}|<\sqrt{3}\hat{\phi}_{qs}$ *and* $\hat{\phi}_{ds}<0$, then sector = S3 (24)

If $|\hat{\phi}_{ds}|\geq\sqrt{3}\hat{\phi}_{qs}$ *and* $\hat{\phi}_{ds}<0$, then sector = S4 (25)

If $|\hat{\phi}_{ds}|\leq\sqrt{3}\hat{\phi}_{qs}$, $\hat{\phi}_{ds}<0$ *and* $\hat{\phi}_{qs}<0$, then sector = S5 (26)

If $|\hat{\phi}_{ds}|<\sqrt{3}\hat{\phi}_{qs}$, $\hat{\phi}_{ds}\geq 0$ *and* $\hat{\phi}_{qs}<0$, then sector = S6 (27)

3.6 Machine Model of an IPMSM

In the analysis and simulation of the IPMSM drive system, the basic equations of IPMSM are used in instantaneous form. By Park's transformation [3-4], the equations of the IPMSM in a rotor reference frame are denoted by the superscript "r," in which the d-axis is aligned with the stator winding of phase "a" and are shown in terms of voltage and flux as follows [3-6],[10-13].

The stator voltage equations are as

$$v_{ds}^r=i_{ds}^rR_s+\frac{d}{dt}\phi_{ds}^r-w_m\phi_{qs}^r \tag{28}$$

$$v_{qs}^r=i_{qs}^rR_s+\frac{d}{dt}\phi_{qs}^r-w_m\phi_{ds}^r \tag{29}$$

These stator voltages are obtained from phase winding voltages (v_{sa} , v_{sb} and v_{sc}) using the Park's transformation as

$$v_{ds}^r=\left(\frac{2}{3}\right)\{v_{sa}\cos\theta_r+v_{sb}\cos(\theta_r-2\pi/3)+v_{sc}\cos(\theta_r-4\pi/3)\} \tag{30}$$

$$v_{qs}^r=\left(\frac{2}{3}\right)\{v_{sa}\sin\theta_r+v_{sb}\sin(\theta_r-2\pi/3)+v_{sc}\sin(\theta_r-4\pi/3)\} \tag{31}$$

The stator flux equations are as

$$\phi_{ds}^r=L_di_{ds}^r+\phi_f \tag{32}$$

$$\phi_{qs}^r=L_qi_{qs}^r \tag{33}$$

where L_d, L_q are the d, q axis inductances respectively and ϕ_f is the stator flux linkage produced by permanent magnets.

By solving equations (28) and (29), the explicit expressions of currents are as

$$i_{ds}^{r} = \int ((v_{ds}^{r} - i_{ds}^{r} R_s + w_m L_q i_{qs}^{r}) / L_d) dt \quad (34)$$

$$i_{qs}^{r} = \int ((v_{qs}^{r} - i_{qs}^{r} R_s - w_m (L_d i_{ds}^{r} + \phi_f)) / L_q) dt \quad (35)$$

These equations (28)-(35) reveal the internal relations among voltage, current and flux of rotor, which can be directly modeled by using SIMULINK blocks. However the above equations are not perfect in building the complete d-q axes motor model; two other equations to reflect the mechanical dynamics should be added.

The electromagnetic torque equation is as

$$T_e = \frac{3P}{4}(\phi_f i_{qs}^{r} + (L_d - L_q) i_{qs}^{r} i_{ds}^{r}) \quad (36)$$

The torque balance equation is as

$$\frac{d}{dt} w_m = \frac{T_e - T_L}{J_m} \quad (37)$$

The phase currents are computed using inverse Park's transformation as

$$i_{sa} = i_{ds} \cos\theta_r - i_{qs} \sin\theta_r \quad (38)$$

$$i_{sb} = i_{ds} \cos(\theta_r - 2\pi/3) - i_{qs} \sin(\theta_r - 2\pi/3) \quad (39)$$

$$i_{sb} = i_{ds} \cos(\theta_r - 4\pi/3) - i_{qs} \sin(\theta_r - 4\pi/3) \quad (40)$$

where θ_r is the position angle of the rotor.

4. Neural Network Based Direct Torque Control Scheme

To reduce the torque ripples and motor current ripples in a conventional DTC, three multilayer feedforward neural networks are used here. These networks emulate the traditional switching table of the DTC of the IPMSM for obtaining the optimal switching patterns. The stator flux-linkage space-vector positions (N) and the results of flux (d_φ) and torque (d_T) controllers determine the switching space vectors of VSI as S_a, S_b, and S_c which are the switching states of the inverter. Since the switching table does not depend on the parameters of the IPMSM, NN may be trained off-line. The output (O/P) of the three networks are the S_a, S_b, and S_c respectively, while the inputs (I/P) d_T, d_φ and N being the same for all three networks. Each NN model is trained for different reference model data set i.e.: the first network deals with [S_a (O/P), d_T, d_φ and N (I/P)], the second one deals with [S_b (O/P), d_T, d_φ and N (I/P)] and the third network deals with [S_c (O/P), d_T, d_φ and N (I/P)], as shown in Fig. 6. Once the networks are trained, the variation in IPMSM parameters would not affect the performance. Each neural network has 36 pairs of input and output patterns for a three level torque controller based DTC and 60 pairs of input and output patterns for a five level torque controller based DTC.

5. Neural Network Structure and Adaptive Algorithm

Three neural networks, each made of three layers, are used to obtain the three output switching states of the inverter S_a, S_b, and S_c simultaneously. Each network having three layers i.e.: input layer, hidden layer and output layer, with a total of 16 tansig neurons, is employed to implement the switching table. The first layer has 15 neurons and the second has one neuron. By utilizing the 60 pairs of input and output patterns for a five level torque controller based DTC, each network is trained by a well-known gradient descent training algorithm [9],[14]. After 241 training epochs, the sum squared error arrives at the minimum. Then the training of the weights is stopped. The NN structure and its adaptive learning algorithm is shown in Fig. 6.

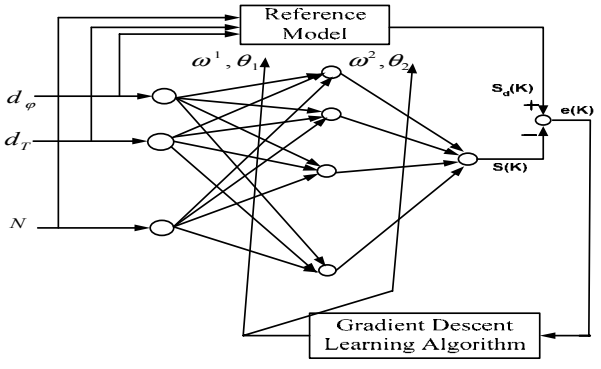

Fig. 6 Neural Network Structure and Its Adaptive Algorithm

General output equation of a neural network is given as

$$S(k) = \Psi_1\left(\sum_{i=1}^{p} \omega_i^2 neu_i(k) + \theta_2\right) \quad (41)$$

where,

$$neu_i(k) = \Psi_2\left(\sum_{j=1}^{3} \omega_{ij}^1 B_j(k) + \theta_1\right) \quad (42)$$

where, $B_1 = d_\varphi$, $B_2 = d_T$, *and* $B_3 = N$. p is the number of nodes in the hidden layer. Ψ_1 and Ψ_2 are activation functions tansig here. k is k^{th} sample which varies from 1 to 60 for a five level torque controller based DTC. θ_1 and θ_2 are biases. ω^1 and ω^2 are the weights between input to hidden layer and between hidden to output layer respectively.

The weights ω^1 and ω^2 are updated by the following equation as

$$\omega_{new}^n = \omega_{old}^n + \Delta\omega^n \text{, where n =1 and 2.} \quad (43)$$

The increment $\Delta\omega^n$ is calculated by gradient descent as

$$\Delta\omega^1 = \eta \frac{\partial J}{\partial \omega^1} = \eta \frac{\partial J}{\partial e} \cdot \frac{\partial e}{\partial S} \cdot \frac{\partial S}{\partial \omega^1} \quad (44)$$

$$\Delta\omega^2 = \eta \frac{\partial J}{\partial \omega^2} = \eta \frac{\partial J}{\partial e} \cdot \frac{\partial e}{\partial S} \cdot \frac{\partial S}{\partial neu} \cdot \frac{\partial neu}{\partial \omega^2} \quad (45)$$

where, η is the fixed leaning rate and J is the performance index which has been taken as mean square error (MSE), as

$$J = \frac{1}{2} ee^T \quad (46)$$

where, $e(k) = S_d(k) - S(k)$, S_d is the desired output and S is the actual output.

6. Neural Network Based Direct Torque Control Scheme

The five level torque controller based DTC using the neural network scheme of an IPMSM has been simulated in Matlab along with Simulink toolbox. Fig. 7(a). Fig. 7(b) and Fig. 7(c) show the Simulink model of the IPMSM and inverter respectively.

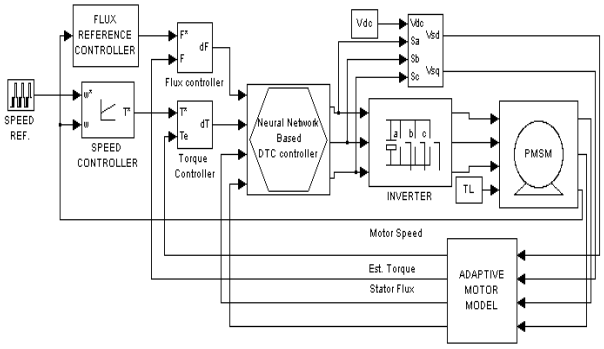

Fig. 7(a) Simulation Model of Neural Network Based DTC

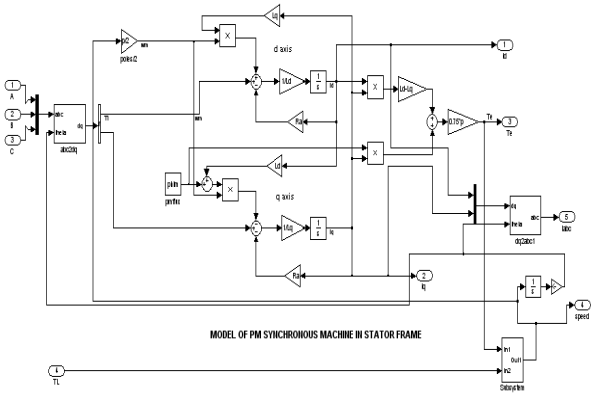

Fig. 7(b) Simulation Model of IPMSM

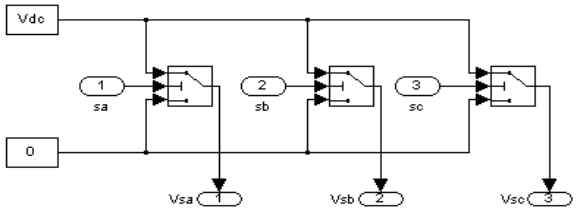

Fig. 7(c) Simulation Model of VSI Inverter

NN has been coded as a Matlab S-function so that it could be run in Simulink. The adaptive motor model estimates the developed torque and stator flux based on the sensing of two stator phase currents and battery voltage. The parameters of the motor used in the simulation are given in the Appendix. The gain constants of PI speed controller are also given in the Appendix.

7. Results and Discussion

Three DTC schemes described earlier have been simulated using Matlab/Simulink.

a) Conventional DTC scheme (Three Level Torque Controller Based DTC).

b) Five Level Torque controller based DTC Scheme

c) Five Level Torque controller based DTC Scheme Using NN

Figs. 8-14 show the speed response, torque response, motor currents and flux response respectively during the starting, acceleration, deceleration (regenerative braking) and above the rated speed for field weakening. The simulation is carried out for the following conditions.

7.1 Transient Response of Vehicle Motor during Starting and Acceleration

The motor is started-up from the zero speed to 200 rad/s and accelerated from 200 rad/s to 400 rad/s at 0.025 second within current/ torque limit and one can observe the variation in the frequency of the currents as the drive accelerates as shown in Fig. 8. From Figs. 8(a)-(c), it is seen that the speed response for various schemes is similar in nature and the estimated speed follows the reference speed closely. Fig. 9(a) shows the torque response of the conventional DTC (scheme (a)) and Fig. 9 (b) shows the response of five level torque controller based DTC (scheme (b)). It is seen that the ripples with scheme (b) have been reduced approximately to half as compared with scheme (a). Fig. 9 (c) shows the torque response of a five level torque controller based DTC using NN (scheme (c)). In scheme (c), the ripples in the torque response are further reduced by half. Figs. 10(a)-(c) show the motor currents for all the schemes. It may be seen that the ripples in the current waveform are drastically reduced. Three phase motor currents are close to sinusoidal and one can observe the variation of the frequency in the currents as the drive speed changes.

7.2 Transient Response of Vehicle Motor during Deceleration (Regenerative braking) and Acceleration of Vehicle above the Rated Speed for Field Weakening

The motor is decelerating from 400 rad/s to 200 rad/s at 0.060 seconds to show the drive behavior during regenerative braking as shown in Fig. 11. When the motor is slowed down during deceleration (regenerative braking), i.e., when the negative torque is applied to the electric vehicle, it behaves as a generator that produces electrical power to recharge the battery. The motor is accelerated from 200 rad/s to 600 rad/s at 0.085 second to show the drive behavior during the above the rated speed for field weakening. The stator flux magnitude is reduced while its frequency is increased when the speed command is above the base speed (for this motor 472 rad/s). The maximum allowable power is reached at base speed. Further acceleration occurs at constant power and the torque decreases inversely with the speed. In the field weakening region, the motor draws a little higher current due to the requirement of maximum torque with the reduced flux. The torque and current response of the vehicle motor during deceleration (regenerative braking) and above the rated speed for field weakening are shown in Fig. 12 and Fig. 13 respectively. Similar reasoning can be made when the vehicle motor operates above the rated speed for field weakening and deceleration (regenerative braking) as explained in section A for starting and acceleration.

Figs. 14(a)-(c) show the DQ-axes flux response for all the schemes. It is appreciated that the flux ripple decreases when the NN is used for a five level torque controller based DTC. It is clearly seen that the ripples in the torque and motor currents respond with a five level torque controller based DTC using the NN (Figs. 9(c) and 10(c)) are drastically reduced. In a five level torque controller based DTC using a neural network (scheme (c)), the ripples of the torque in steady state are reduced remarkably as compared with a conventional DTC (scheme (a)). To further highlight this feature, Table 3 shows the percentage torque ripple for all the schemes during starting, acceleration above the rated speed for field weakening and deceleration (regenerative braking).

Table 3 Comparison of Percentage Torque Ripple of IPMSM Drive

Speed (rad/s)	Conventional DTC	Five level torque controller DTC	Five level torque controller Based DTC using NN
Starting(0-200)	8.47 %	2.97 %	0.74 %
Acceleration(200-400)	8.05 %	2.75 %	0.85 %
Regenerative braking(400-200)	8.05 %	2.54 %	0.74 %
Above rated speed for field weakening (200-600)	7.83 %	3.35 %	1.05 %

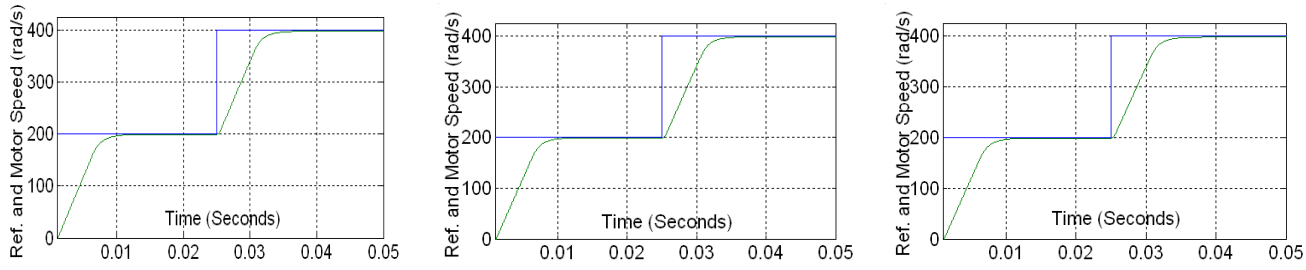

Fig. 8 Speed response of vehicle motor during starting, and acceleration (a) Conventional DTC scheme (b) Five level torque controller based DTC scheme (c) Five level torque controller based DTC using NN scheme

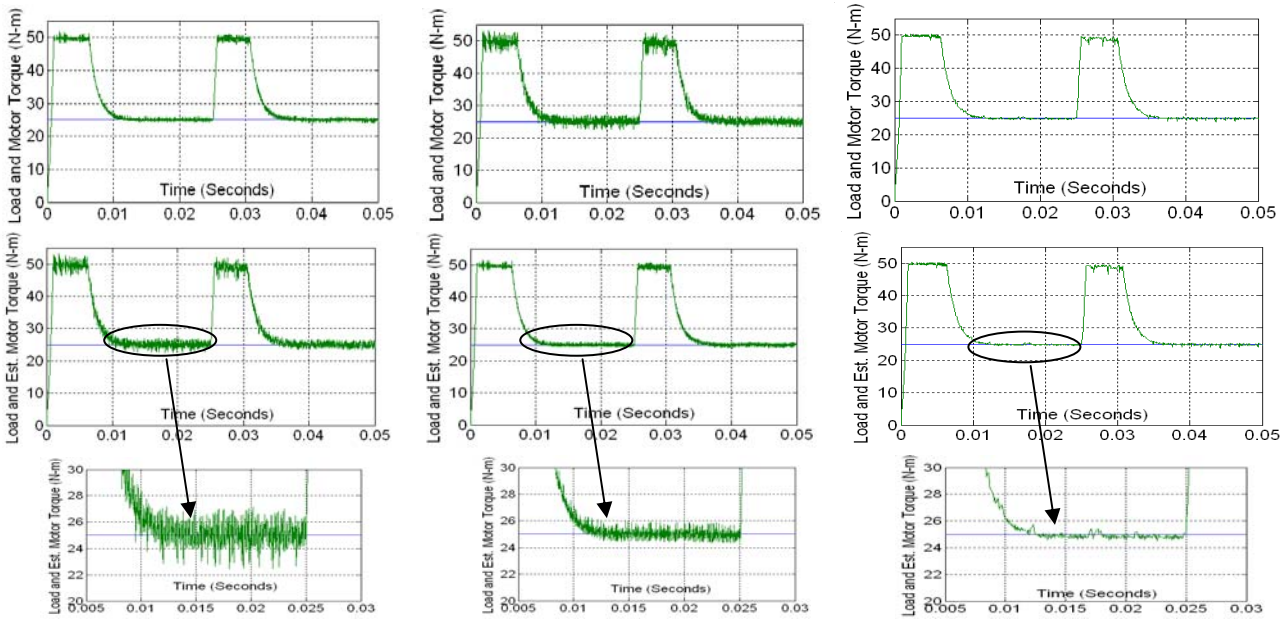

Fig. 9 Torque response of vehicle motor during starting, and acceleration (a) Conventional DTC scheme (b) Five level torque controller based DTC scheme (c) Five level torque controller based DTC using NN scheme

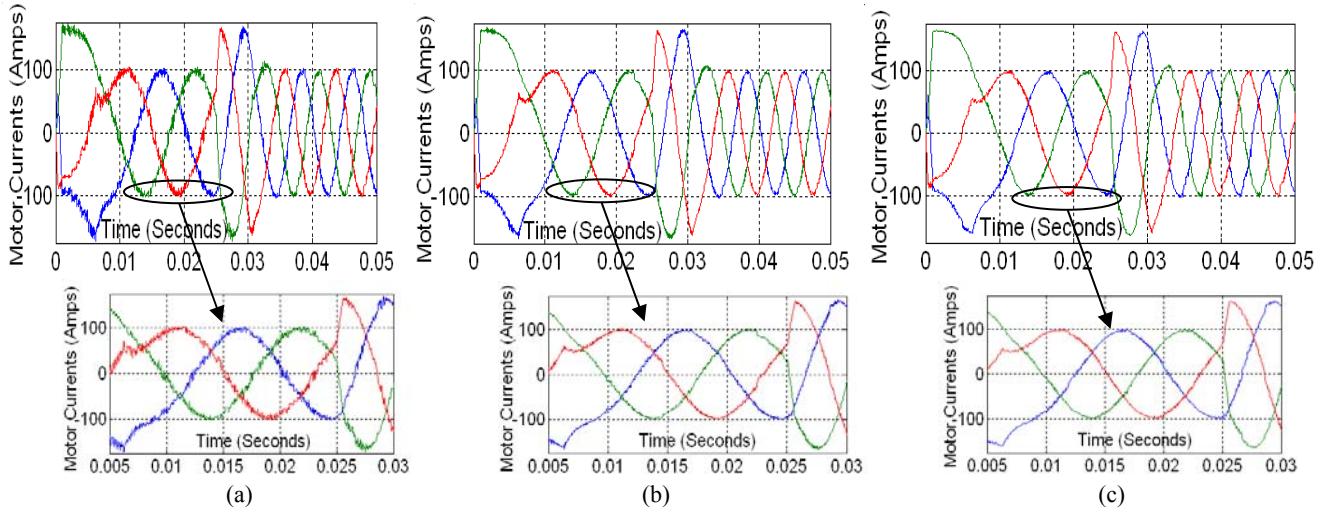

Fig. 10 Motor current response of vehicle motor during starting and acceleration (a) Conventional DTC scheme (b) Five level torque controller based DTC scheme (c) Five level torque controller based DTC using NN scheme

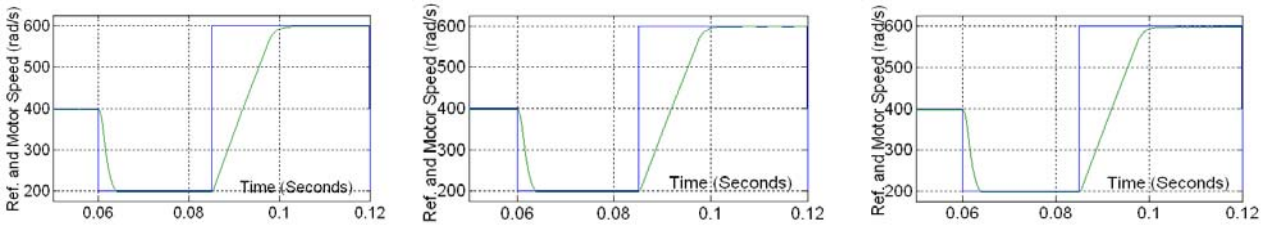

(a) (b) (c)

Fig. 11 Speed response of vehicle motor during deceleration (regenerative braking) and above the rated speed for field weakening (a) Conventional DTC scheme (b) Five level torque controller based DTC scheme (c) Five level torque controller based DTC using NN scheme

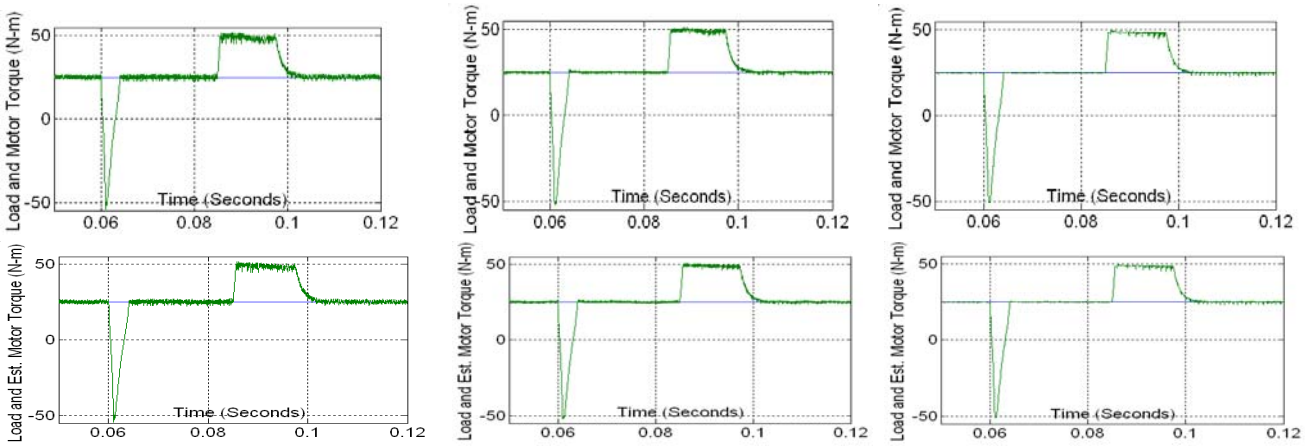

(a) (b) (c)

Fig. 12 Torque response of vehicle motor during deceleration (regenerative braking) and above the rated speed for field weakening (a) Conventional DTC scheme (b) Five level torque controller based DTC scheme (c) Five level torque controller based DTC using NN scheme

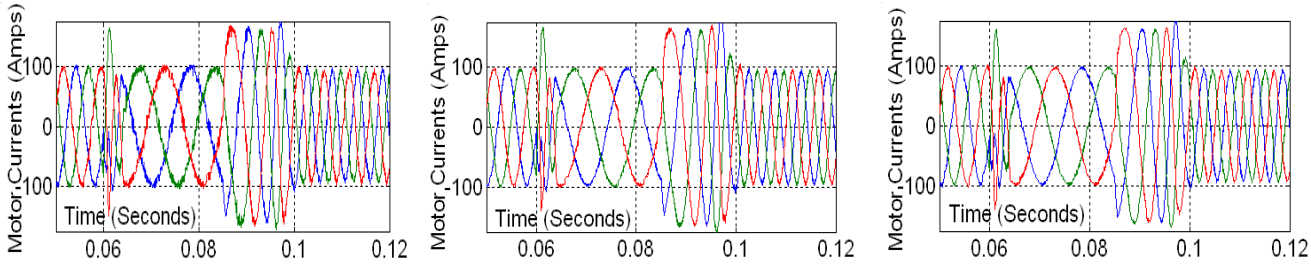

(a) (b) (c)

Fig. 13 Motor current response of vehicle motor during deceleration (regenerative braking) and above the rated speed for field weakening (a) Conventional DTC scheme (b) Five level torque controller based DTC scheme (c) Five level torque controller based DTC using NN scheme

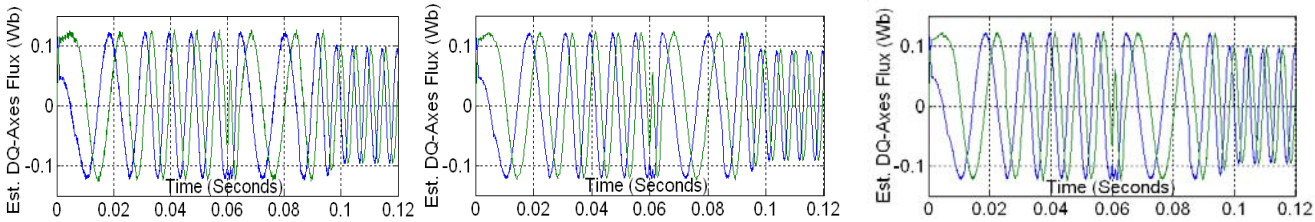

(a) (b) (c)

Fig. 14 DQ-axes flux response of vehicle motor during starting, acceleration, deceleration (regenerative braking) and above the rated speed for field weakening (a) Conventional DTC scheme (b) Five level torque controller based DTC scheme (c) Five level torque controller based DTC using NN scheme

Comparison of the results shows that the proposed five level torque controller based DTC using the NN is superior to the other schemes with respect to the steady state torque ripples. The ripples in the flux and motor currents are also decreased in case of a five level torque controller based DTC using the NN. These results demonstrate the effectiveness of a neural network on DTC scheme.

8. Conclusion

A comparison of various direct torque control methodologies of the IPMSM have been made in order to evaluate the influence of the motor operating condition on a steady state performance. It has been found that there is an approximate 90% reduction in the motor current and torque ripples in a NN based five level torque controller DTC as compared to the conventional DTC. Besides, it is clear that such controllers have been found to provide the desired dynamics. The improved steady-state performance has been achieved in a neural network based DTC of IPMSM for a wide range of speed control. With these advantages, the proposed NN based five level torque controller DTC scheme may be used in the electric vehicle propulsion system.

Appendix

Motor and speed controller specifications:
Interior Permanent magnet synchronous motor (IPMSM) Parameters [15]:
22 kW, R_s = 40.4 mΩ, P = 4, ϕ_f = 0.08764 Wb.
L_d = 0.4456 mH, L_q = 0.8276 mH, W_{base} = 4500 rpm.
PI Controller: K_P = 1.0, K_I = 0.05.

References

[1] C. Chan, "The State of the Art of Electric and Hybrid Vehicles," *Proc. of IEEE*, vol. 90, no. 2, pp. 247--275, Feb. 2002.

[2] J. Faiz, M. B. B. Sharifian, Ali Keyhani, and A. B. Proca, "Sensorless Direct Torque Control of Induction Motors Used in Electric Vehicle," *IEEE Trans. Energy Conversion*, vol. 18, no. 1, pp. 1-10, March. 2003.

[3] P. Vas, "*Sensorless Vector and Direct Torque Contro,l"* Oxford University Press, London, U.K., 1998.

[4] B. K. Bose, "*Modern Power Electronics and AC Drives,*" IEEE Press, New York 2003.

[5] L. Tang, L. Zhong, M.F. Rahman and Y. Hu, "Novel Direct Torque Controlled Interior Permanent Magnet Synchronous Machine Drive With Low Ripple in Flux and Torque and Fixed Switching Frequency," *IEEE Trans. on Power Electronics*, vol. 19, no.2, pp. 346-354, March 2004.

[6] L. Lianbing, S. Hexu, W. Xiaojun and T. Yongquing, "A High-Performance Direct Torque Control Based on DSP in Permanent Magnet Synchronous Motor Drive," *in Proc IEEE ICA'02*, 2002, pp. 1622-1625.

[7] I. Takahashi and T. Noguchi, "A New Quick-Response and High-Efficiency Control Strategy of an Induction Motor," *IEEE Trans.Ind Apl*, vol. IA-22, no. 5, pp. 820-827, Sept./Oct. 1986.

[8] Yen-Shin Lai, Wen-Ke Wang and Yen-Chang Chen, "Novel Switching Techniques for Reducing the Speed Ripple of AC Drives With Direct Torque Control," *IEEE Trans. on Ind. Electronics*, vol. 51, no. 4, pp. 768-775, Aug. 2004.

[9] K. L. Shi, T. F. Chan, Y. K. Wong, S. L. Ho, "Direct Self Control of Induction Motor Based on Neural Network," *IEEE Trans. on Ind. App*, vol. 37, no. 5, pp. 1290-1298, Sep./Oct. 2001.

[10] L. Zhong, M. F. Rahman, W. Y. Hu, K. W. Lim, "Analysis of Direct Torque Control in Permanent Magnet Synchronous Motor Drives," *IEEE Trans. on Power Electronics*, vol. 12, no. 3, pp. 528-536, May 1997.

[11] P. Pillay and P. Freere, "Literature Survey of Permanent Magnet AC Motor and Drive," in *Proc. IEEE IAS'89,* vol. 1, pp.74-84, 1889.

[12] P. Pillay and R. Krishnan, "Modeling of Permanent Magnet Motor Drives," *IEEE Trans. on Ind. Electronics*, vol. 35, no. 4, pp. 537-541, Nov. 1998.

[13] T. J. E. Miller, "*Brushless Permanent Magnet and Reluctance Motor Drives,"* Oxford Science Publication, U.K., 1989.

[14] J. M. Zurada, "*Introduction to Artificial Neural Systems*, West Publishing," St. Paul, MN (Editor), 1992.

[15] J. W. Park, D. H. Koo, J. M. Kim, and H. G. Kim, "Improvement of Control Characteristics of Interior Permanent Magnet Synchronous Motor for Electric Vehicle," *IEEE Trans. on Ind. Electronics*, vol. 37, no. 6, pp. 1754-1760, Nov./Dec. 2001.

Bhim Singh was born in Rahamapur, U. P., India in 1956. He received his B. E. (Electrical) degree from the University of Roorkee, India in 1977 and his M. Tech. and Ph. D. degrees from Indian Institute of Technology (IIT), New Delhi, in 1979 and 1983, respectively. In 1983, he joined as a Lecturer and in 1988 became a Reader in the Department of Electrical Engineering, University of Roorkee. In December 1990, he joined as an Assistant Professor, became an Associate Professor in 1994 and Professor in 1997 at the Department of Electrical Engineering, IIT Delhi, India. His field of interest includes power electronics, electrical machines and drives, active filters, static VAR compensator, analysis and digital control of electrical machines. Dr. Singh is a Fellow of Indian National Academy of Engineering (INAE), Institution of Engineers (India) (IE (I)) and Institution of Electronics and Telecommunication Engineers (IETE). He is also a Life Member of Indian Society for Technical Education (ISTE), System Society of India (SSI) and National Institution of Quality and Reliability (NIQR), as well as a Senior Member IEEE (Institution of Electrical and Electronics Engineers).

Pradeep Jain graduated from M. M. Eng. College in 2000 with a B. Tech. degree, a M. Tech. in Process Control from Netaji Subhas Institute of Technology, Delhi in 2002 and is presently pursuing his Ph.D. He is currently working as a Teaching cum Research Fellow in Netaji Subhas Institute of Technology. His research interests include electric vehicle propulsion system, electric drives and power electronics.

A.P.Mittal graduated in 1978 from M.M. Eng. College, Gorakhpur with his M.E. in 1980 from the University of Roorkee and his PhD in 1991 from IIT Delhi. He has more than twenty years of teaching experience and is presently a Professor and Head of Instrumentation and Control Engineering Division in Netaji Subhas Institute of Technology. He is a Fellow of Institution of Engineers (India) and a senior member of Institution of Electrical and Electronics Engineers. His research interests include power electronics, FACTS, active filters and electric drives.

J.R.P Gupta graduated from Muzaffarpur Institute of Technology (M.I.T) and received his B.Sc. degree in 1972 and completed his Ph.D. degree from the University of Bihar in 1983. He has teaching experience of more than twenty five years. He has more than twenty five years of teaching experience. He has been in the Netaji Subhas Institute of Technology for the last ten years and is presently holding the position of Professor in Instrumentation and Control Engineering Department. His research interests include power electronics, electric drives, and power quality.